Journal of Engineering Physics and Thermophysics, Vol. 82, No. 4, 2009

INFLUENCE OF PARTICLE DENSITY AND SIZE ON TURBULENCE, FRICTION, AND HEAT EXCHANGE CHARACTERISTICS

K. N. Volkov and V. N. Emel'yanov

UDC 532.529

Numerical simulation of turbulent flows of a gas suspension in the vicinity of the critical point and in a channel with permeable walls has been carried out. The influence of the concentration of the dispersed phase and the size of its particles on the distribution of mean and pulsation characteristics of the flow, as well as on the friction and heat transfer coefficients, is discussed.

Keywords: *turbulence, particle, flow, friction, numerical simulation, critical point, injection channel.*

Introduction. The investigation of the behavior of solid particles in a turbulent flow and their influence on the local and integral characteristics of the flow is an important problem in the mechanics of two-phase media.

The specific features of the particle motion in a turbulent flow and the intensity of interphase processes depend on the inertia of particles (Stokes number) and the impurity concentration [1, 2]. The gradient character of the profiles of the average and pulsation parameters of the gas leads to an inhomogeneity of the force factors acting on the particle, which leads to the formation of inhomogeneous profiles of the average and pulsation parameters of the dispersed phase.

The low-inertia particles present in an equilibrium flow at $\mathrm{Stk} \to \infty$ completely follow turbulent pulsations of the carrier flow velocity and are able to react to a change in its parameters. The mean and pulsation velocity profiles of such particles follow the corresponding velocity profiles of the gas phase. With increasing impurity concentration the influence of particles on the gas increases.

In frozen flow, at $\mathrm{Stk} \to \infty$ particles do not react to turbulent pulsations of the carrier flow velocity, and the mean velocity distributions of the dispersed phase are practically homogeneous over the cross-section. Sliding of the phases leads to an intensive momentum exchange between the gas and the particles, causing filling of the mean velocity profile of the gas.

The quasi-equilibrium flow at $\mathrm{Stk} = O(1)$ is characterized by the equality of the mean velocities of the gas and dispersed phases. Unlike the equilibrium flow, the inertia of particles is sufficient for the pulsation velocities of the gas and the particles to have a different value. The turbulence intensity of the carrier flow with increasing impurity concentration decreases, which leads to its laminarization and a decrease in the filling of the mean velocity profile of the gas phase.

Investigations of gas-dispersed jets have shown that the presence of particles leads to a decrease in the turbulence intensity, Lagrangian rescaling, and a change in the energy spectrum of turbulence, as well as to a suppression of its high-frequency components [1].

In nonequilibrium flows at arbitrary Stokes numbers the presence of relatively low-inertia particles leads to a suppression of the turbulence intensity of the carrier flow (this influence increases with increasing impurity concentration). The reason for the suppression of turbulent pulsations by particles is their involvement in the pulsation motion as a result of the interaction with turbulent vortices. The maximum quenching of pulsations of the longitudinal and transverse velocities is observed near the channel axis, and the degree of suppression of turbulence increases as the mass concentration of the dispersed phase of particles increases and their inertia decreases. There is a tendency for a shift of the maximum in the pulsation distribution of the transverse velocity of the gas phase in the direction of the wall compared to the distribution in pure gas [3].

D. F. Ustinov Baltic State Technological University "Voenmekh," 1st Krasnoarmeiskaya Str., St. Petersburg, 190005, Russia. Translated from Inzhenerno-Fizicheskii Zhurnal, Vol. 82, No. 4, pp. 758–766, July–August, 2009. Original article submitted November 26, 2007.

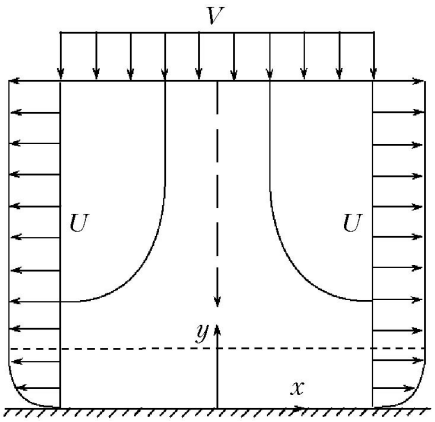

Fig. 1. Coordinate system.

The results of the physical experiment of turbulent flows of a gas suspension in a channel and in a homogeneous shear layer [4], as well as the kinetic equation for the probability density function of particle velocities in an inhomogeneous turbulent flow [5], show that pulsations of particle velocities exceed carrier phase pulsations near the channel axis.

In the present paper, numerical simulation of turbulent flows of a gas suspension in the vicinity of the critical point and in a channel with permeable walls has been carried out. We have investigated the influence of the dispersed phase concentration, the size of particles, and the thermal properties of the gas and dispersed phases on the distribution of the average and pulsation characteristics of the flow, as well as on the friction and heat transfer coefficients.

Mathematical Model. The turbulent flow of the gas suspension is described by the equations of a two-velocity and two-temperature medium. The flow is assumed to be quasi-stationary, and the carrier phase incompressible with constant thermal properties. Terms describing the heat release due to the work of the viscous forces and the interphase interaction forces, as well as terms containing pulsations of the transfer and pressure coefficients, are ignored. The tensor components of Reynolds stresses are calculated on the basis of the Kolmogorov–Boussinesq hypothesis and the turbulent viscosity concept, for whose calculation the Kolmogorov–Prandtl formula is used.

The dispersed phase is modeled by a continuum having no natural stresses. The interphase interaction model takes into account the hydrodynamical drag force. The drag coefficient is calculated by the Stokes law. The intensity of interphase momentum and energy exchange is defined as the product of the countable particle concentration by the rate of interphase exchange per one particle.

To close the basic equations, the k–ε model of turbulence is used. The influence of the dispersed phase is taken into account by means of additional source terms [1, 2] calculated according to the hypothesis of local isotropy of dissipating vortices and inhomogeneity of the mean velocity field of the dispersed phase.

To calculate the correlation moments connected with the dispersed phase, we use the locally homogeneous approximation to the method of space-time averaging with step approximation of the Euler correlation function of velocity pulsations of the carrier flow along the particle path [1]. The difference in turbulence scales in the longitudinal and transverse directions is taken into account by means of the locally homogeneous and locally isotropic turbulence theory [6].

To simplify the problem solution, it is assumed that the distributions of the flow characteristics in different areas differ only in the scales of length and velocity. A solution is sought in a form for which the longitudinal velocities of the gas and particles depend linearly on the x coordinate, and the other unknowns are a function of the y coordinate alone. The equations describing the turbulent flow of the gas suspension are reduced to a closed system of nonlinear ordinary differential equations whose form is given in [7] (flow in the vicinity of the critical point) and in [8] (flow in a channel with permeable walls).

Flow in the Vicinity of the Critical Point. Let us consider the flow of a viscous incompressible liquid with discrete particles past a smooth blunt body. The origin of the coordinate is at the stagnation point of the flow. The x and y axes are directed along the wall and normal to the barrier surface. The y coordinate is positive in the direction opposite to the direction of the incident flow (Fig. 1).

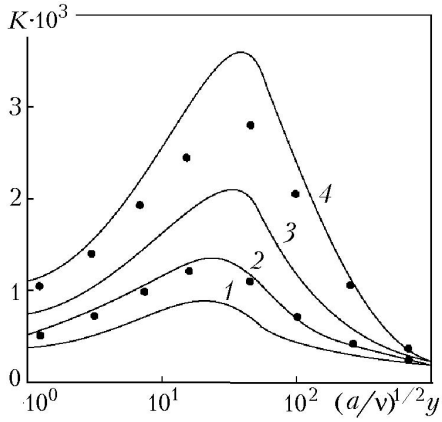

Fig. 2. Kinetic turbulence energy distributions at Re = $5 \cdot 10^4$ (1); 10^5 (2); $2 \cdot 10^5$ (3); $5 \cdot 10^5$ (4). Dots correspond to the data of [9].

Boundary conditions. The flow at the outer boundary of the calculation domain is assumed to be equilibrium with respect to the velocity and temperature. For the mean velocity on the wall, the adhesion and nonpercolation conditions are given, and for the temperature, the wall temperature is given. The kinetic turbulence energy is assumed to be equal to zero on the barrier surface.

Velocity and temperature distributions. The average temperature profile in the boundary layer depends on the Reynolds number and the degree of turbulence, whereas the mean longitudinal velocity distribution differs insignificantly from the solution for the laminar boundary layer in the vicinity of the stagnation point. A comparatively rapid growth of the velocity and temperature takes place inside the viscous sublayer.

The calculated longitudinal velocity and temperature distributions of the gas in the boundary layer thickness for different flow conditions point to higher gradients of the gas-dynamic parameters of the carrier flow near the wall compared to the pure gas flow. The change in the velocity and temperature fields of the gas phase is due mainly not to the interphase momentum and heat exchange but to the decrease in the thicknesses of the dynamic and thermal boundary layers in a dusty flow. The influence of the particle size on the gas velocity and temperature distributions is insignificant.

The longitudinal velocity profile of the dispersed phase depends, apart from the external flow parameters, on the Stokes number and, to a lesser extent, on the degree of impurity concentration. Near the wall the particle velocity is higher, and in the flow core it is lower than the gas velocity. This means that particles slide by the gas downstream (near-wall region) or upstream against the flow (flow core).

Distribution of turbulence characteristics. The distributions of the kinetic turbulence energy and its dissipation velocity in the pure gas flow are given in Fig. 2 at $\theta \mathrm{Re}^{1/2} = 20$. As a typical scale of velocity, the quantity $(\nu a)^{1/2}$ is chosen.

The Reynolds number and the turbulence intensity have an effect on the results of calculations by changing the extent of the viscous domain in dimensionless coordinates. Comparison with the results of [9] shows that the model constructed gives overestimated values of the kinetic turbulence energy (Fig. 2) but is in good agreement with [9] for the gas velocity.

Particles produce a double effect on the turbulence characteristics near the wall. On the one hand, there occurs additional, with respect to the pure gas turbulent flow, dissipation of kinetic turbulence energy and turbulence suppression, and, on the other hand, the particles decrease the boundary layer thickness, thus increasing the mean velocity gradient of the gas phase near the wall, which leads to additional generation of turbulence.

The solutions presented in Fig. 3 show that the presence of particles leads to a suppression of turbulent pulsations near the wall and a quenching of turbulence. The results are normalized to the maximum value of the kinetic energy in the pure gas flow K_0. The curves in Fig. 3a correspond to $\alpha_p = 10^{-4}$ and $r_p = 5$ μm (curve 2), 10 μm (curve 3), 15 μm (curve 4), and 25 μm (curve 5). Curve 1 corresponds to the flow without particles. The results shown in Fig. 3b correspond to $r_p = 5$ μm and $\alpha_p = 0$ (curve 1), $5 \cdot 10^{-5}$ (curve 2), 10^{-4} (curve 3), and $2 \cdot 10^{-4}$ (curve 4).

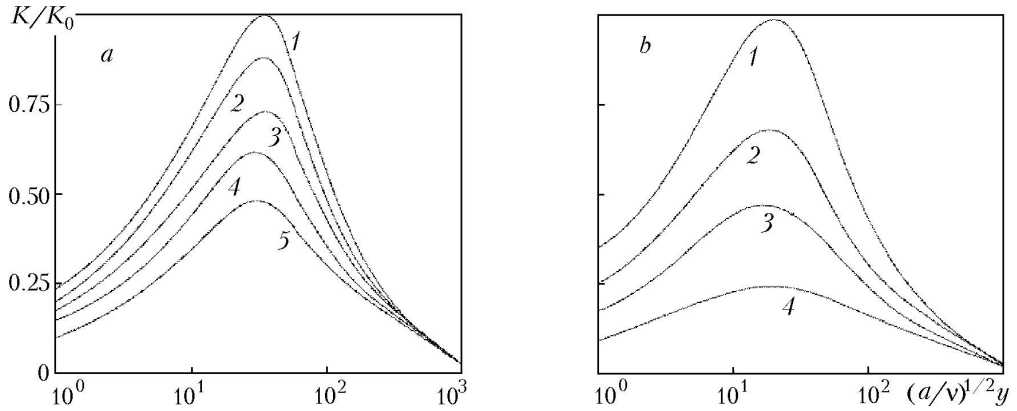

Fig. 3. Kinetic turbulence energy distribution depending on the particle size and the dispersed phase concentration.

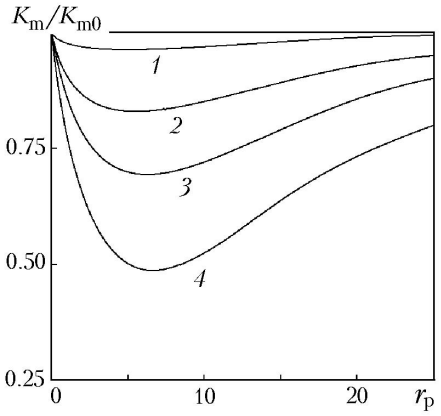

Fig. 4. Influence of the particle size and the dispersed phase concentration on the maximum value of the kinetic turbulence energy at $\alpha_p = 10^{-5}$ (1); $5\cdot10^{-5}$ (2); 10^{-4} (3); $2\cdot10^{-4}$ (4). r_p, μm.

At $\alpha_p < 2\cdot10^{-5}$ the influence of the dispersed phase on the turbulence field becomes small and the additional dissipative terms in the equations of the k–ε model of turbulence play no important role.

The dependences of the maximum values of the kinetic turbulence energy in the two-phase flow on the particle density and size are given in Fig. 4. The dependence of the kinetic turbulence energy on the particle size has a minimum at r_p = 6 μm. The presence of small particles leads to a lowering of the level of turbulence near the wall. Fairly large particles have a less effective influence on the appearance of turbulence near the wall.

Friction and heat transfer. With increasing degree of turbulence and Reynolds number the surface friction and heat transfer coefficients increase. The results of the calculations point to a stronger influence of the turbulent incident flow on the heat exchange in the vicinity of the critical point than on the friction.

The influence of the degree of turbulence on the heat transfer intensification coefficient is shown in Fig. 5. Dots correspond to the data of [10]. The results are normalized to the heat transfer coefficient at θ = 0. Curve 1 in Fig. 5a corresponds to the calculation data, and curve 2 corresponds to the dependence of [11]. The data in Fig. 5b were obtained at Re = 10^4 (curve 1), 10^5 (curve 2), and 10^6 (curve 3).

At large Reynolds numbers a decrease in the boundary layer thickness promotes a deeper penetration into it of turbulent pulsations, which makes it susceptible to perturbations coming from the external flow; therefore, the heat transfer coefficient increases. Such a character of the dependence also takes place in the two-phase flow, but with increasing Reynolds number the intensifying effect of the dispersed phase decreases.

The interaction of particles with the near-wall region of the flow and the change in the gas temperature and velocity distributions near the wall are responsible for the intensification of the heat transfer to the wall and the increase in the surface friction stress in the two-phase flow compared to the pure gas flow.

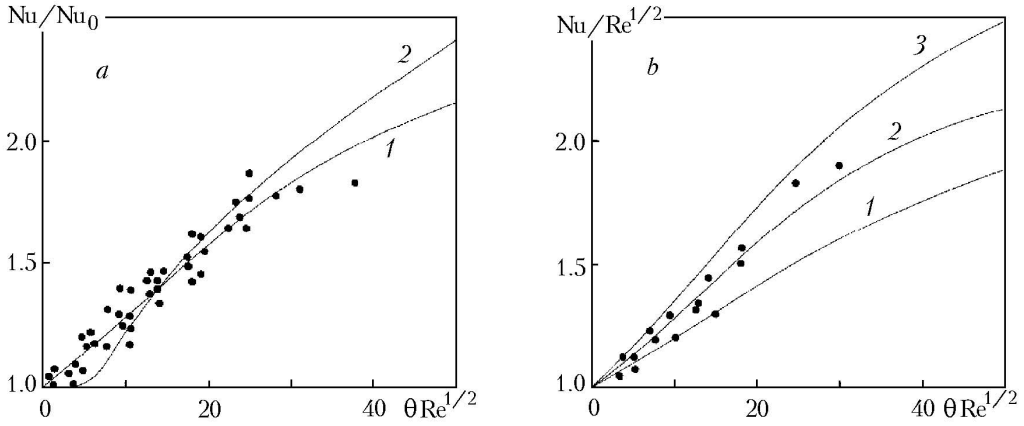

Fig. 5. Influence of the degree of turbulence on the heat transfer intensification coefficient. Dots correspond to the data of [10].

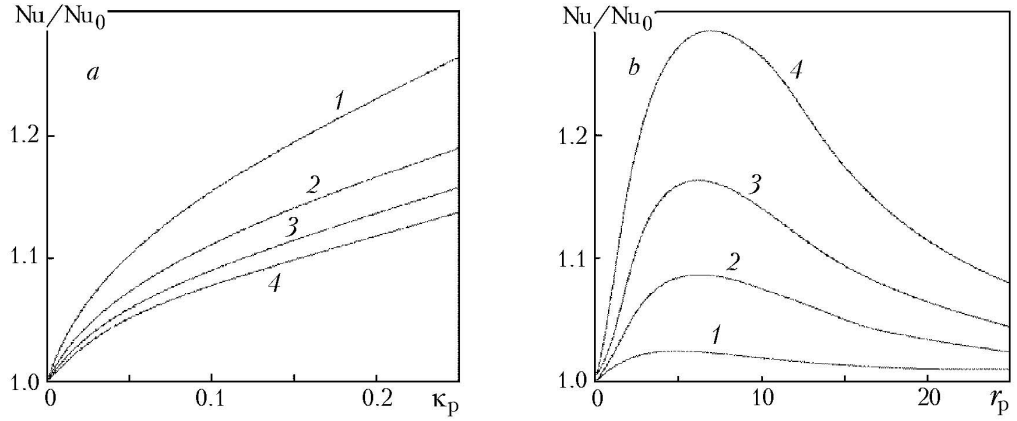

Fig. 6. Influence of the particle size and the dispersed phase concentration on the heat transfer intensification coefficient. r_p, μm.

In the two-phase flow, the migration of particles to the wall leads to additional turbulent energy transfer from the flow core into the viscous layer, weakening the effect of the decrease in the intensity of pulsation motion of the carrier phase and to additional mean motion momentum transfer to the wall increasing the friction stress.

The results of calculations processed in the form of the dependence of the Reynolds number on the mass concentration and size of particles are presented in Fig. 6. The coefficient of intensification of the heat exchange is defined as the ratio between the heat transfer coefficients in the two-phase Nu and pure gas Nu_0 flows with all other parameters being equal. The data in Fig. 6a correspond to r_p = 5 μm (curve 1), 10 μm (curve 2), 15 μm (curve 3), and 25 μm (curve 4). The curves in Fig. 6b correspond to the values of $\alpha_p = 10^{-5}$ (curve 2), $5 \cdot 10^{-5}$ (curve 2), 10^{-4} (curve 3), and $2 \cdot 10^{-4}$ (curve 4).

As the mass concentration of the discrete component increases, a tendency for an increase in the relative level of friction and heat transfer is observed. For small particles they increase to a greater extent than for larger ones, since turbulent migration of small particles to the wall leads to additional turbulent transfer of the momentum of mean motion to the viscous sublayer (in the direction of the wall), weakening the effect of decrease in the intensity of pulsation motion of the gas in flows with sufficiently small particles.

In the laminar flow, the intensification of the heat exchange is explained by the increase in the temperature gradient of the gas phase near the wall. The difference between the heat transfer and friction coefficients in the laminar and turbulent flows of the gas suspension is about 16 and 12%, respectively.

The basic thermophysical parameters influencing the heat transfer between the gas suspension flow and the wall are the density and heat capacity ratios between the gas and dispersed phases.

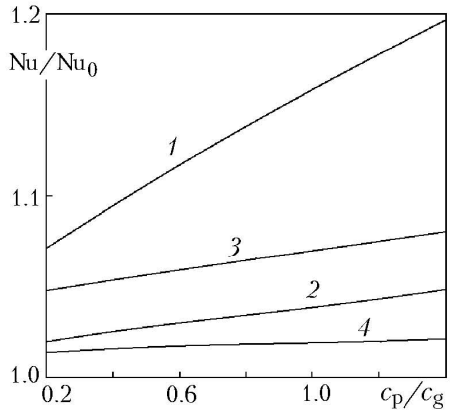

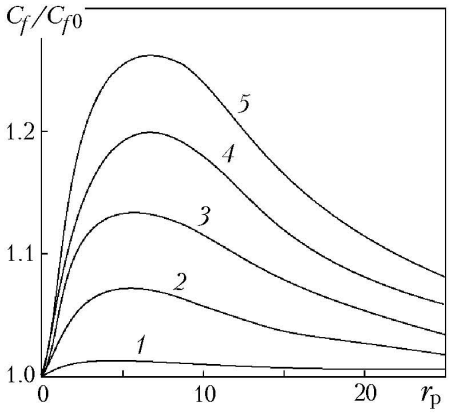

Fig. 7. Influence of the heat capacity ratio between the phases on the heat transfer in the two-phase flow depending on the dispersed phase concentration and the particle size at $\kappa_p = 0.52$ (1, 3) and 0.1 (2, 4). $r_p = 5$ μm and 15 μm (3, 4).

Fig. 8. Influence of the mass concentration and size of particles on the surface friction increase coefficient at $\alpha_p = 10^{-5}$ (1); $5\cdot10^{-5}$ (2); 10^{-4} (3); $1.5\cdot10^{-4}$ (4); $2\cdot10^{-4}$ (5). r_p, μm.

Of greatest interest is the elucidation of the dependence of the heat transfer coefficient on the heat capacity ratio between the phases (Fig. 7), which determines the contribution of the dispersed phase to the turbulent heat transfer in the dusty flow. For small particles participating in the turbulent heat transfer and influencing more effectively the properties of the boundary layer, the influence of the heat capacity ratio between the phases is stronger than for large particles. At $r_p > 20$ μm the influence of this criterion is weak at any impurity concentration.

The influence of the ratio of real phase densities on the heat transfer intensification coefficient in the dusty gas flow is analogous to and as strong as the influence of the heat capacity ratio between the phases.

On the basis of sampled data of the computing experiment we have obtained by the multifactor regression method the functional dependence of the heat transfer intensification coefficient on the parameters of the gas and dispersed phases:

$$\frac{\mathrm{Nu}}{\mathrm{Nu}_0} = 1 + C\left(\frac{r_p}{R}\right)^{-0.466} \kappa_p^{0.607}\left(\frac{c_p}{c_g}\right)^{0.223},$$

where $C = 2.73\cdot10^{-3}$. The given relation finds confirmation at $\frac{r_p}{R} = (5\text{–}50)\cdot10^{-5}$, $\kappa_p = 0.\text{–}0.42$, $\frac{c_p}{c_g} = 0.1\text{–}1.5$.

The exponent with which the particle density enters into the majority of empirical formulas is always less than 0.8, and in flows with small particles the influence of their density is weaker than with large particles. According to the data of [12], for particles with $r_p < 32$ μm their density increases the Nusselt number as $\kappa_p^{0.33}$, and according to the data of [1], as $\kappa_p^{0.45}$, whereas for larger particles the exponent is equal to 0.25.

The influence of various factors on the surface friction coefficient is weaker than on the Nusselt number, especially in the range of 5 μm $< r_p <$ 10 μm (Fig. 8). The friction coefficient distribution depending on the particle size is not monotonous and has a maximum tending to shift towards larger particles with increasing concentration of the dispersed phase.

Flow in the Injection Channel. Consider a quasi-developed flow in a long plane or cylindrical channel of half-width or diameter h when the flow characteristics referred to the velocity on the channel axis vary slightly along its length [8]. Let us align the x with the plane or the symmetry axis of the channel and direct the y axis perpendicularly to it (Fig. 9). The injection velocity v_w is assumed to be equal at all points of the permeable surface of the chan-

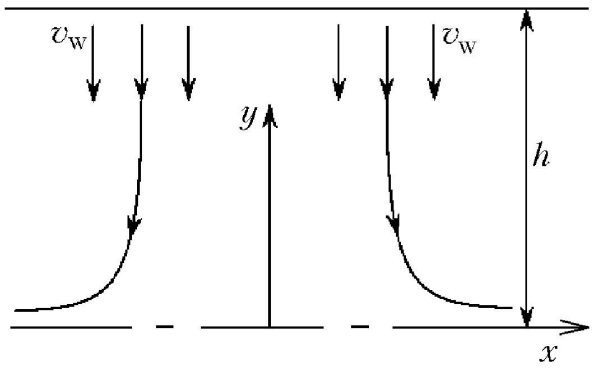

Fig. 9. Flow in the permeable-wall channel.

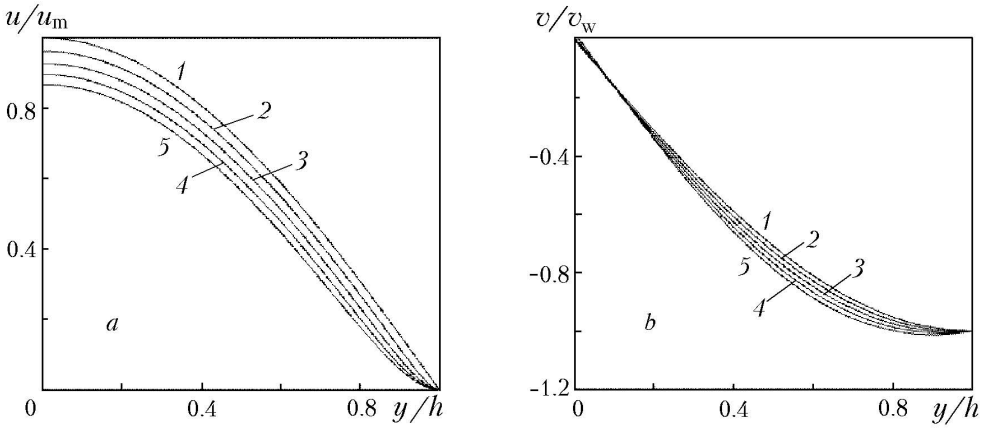

Fig. 10. Distributions of the longitudinal (a) and transverse (b) velocities of the gas (1) and dispersed phases at Stk = 0.025 (2); 0.05 (3); 0.075 (4); 0.1 (5).

nel and directed perpendicularly to it. It is assumed that the liquid spreads symmetrically about the plane $x = 0$. The solution depends on the parameter $M = 1/u_m$ and the Reynolds number $\mathrm{Re} = v_w h/\nu$.

Boundary conditions. On the plane or on the symmetry axis of the channel (at $y = 0$) the flow symmetry conditions are given. On the permeable wall (at $y = h$) for the velocities of the gas and dispersed phases the conditions of normal injection ($u = u_p = 0$, $v = v_p = -v_w$) are given. For the thermal boundary condition, the wall temperature is given. For turbulence characteristics, the condition of the absence of velocity pulsations on the permeable surface of the channel is taken.

Velocity distribution. The velocity distributions of the gas and dispersed phases are given in Fig. 10. The longitudinal velocity profile of the dispersed phase is less filled compared to the velocity profile of the carrier flow (Fig. 10a). The transverse velocity distributions of the dispersed phase differ relatively slightly from one another (Fig. 10b).

With increasing injection intensity the influence of viscous effects on the structure of the turbulent flow weakens and manifests itself mainly in the near-axis region leading to an insignificant filling of the velocity profile. In the plane channel, with increasing Reynolds number the longitudinal velocity profile becomes more prolate and tends to a cosine distribution [13] at strong injection ($\mathrm{Re} \to \infty$). In the axially symmetric flow, with increasing injection intensity the longitudinal velocity distribution becomes less filled.

The distribution of shear stresses in the presence of injection differs from the linear dependence that takes place in a channel with solid walls. The maximum of shear stresses shifts from the wall into the flow, and its value increases with increasing injection intensity.

Distributions of turbulence characteristics. The specific feature of the flow in a distributed-mass-supply channel is the presence of a negative pressure gradient caused by the flow acceleration due to injection [13], which has a strong effect on the mechanism and intensity of turbulent transfer.

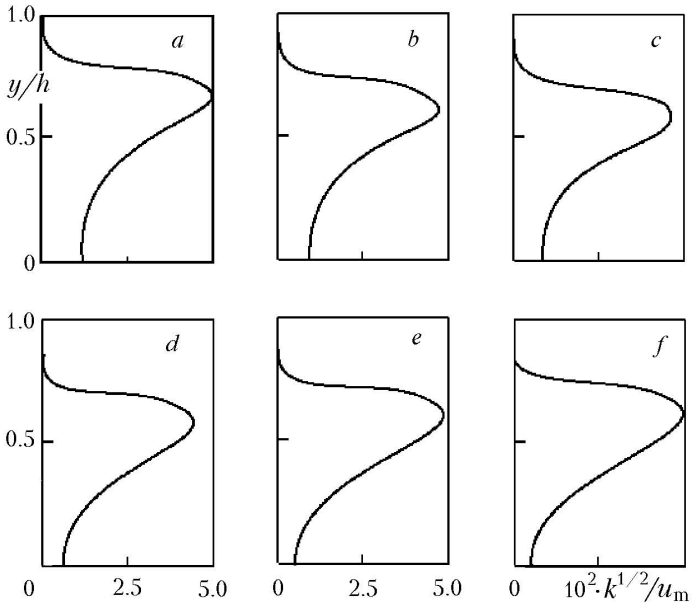

Fig. 11. Kinetic turbulence energy distributions in the intensive-injection channel at M = 0.04 (a); 0.032 (b); 0.02 (c); 0.016 (d); 0.012 (e); 0.01 (f).

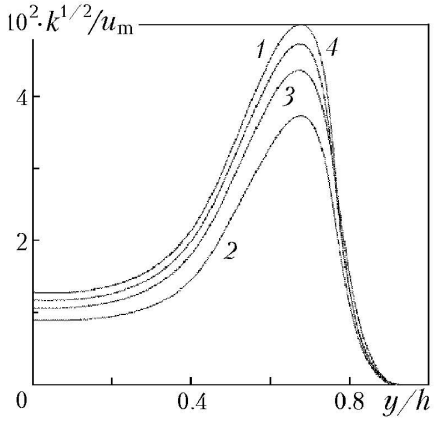

Fig. 12. Kinetic turbulence energy distributions in the intensive-injection channel at M = 0.036 and κ_p = 0.18: 1) pure gas flow; 2) flow with particles of r_p = 5 μm; 3) 10 μm; 4) 15 μm.

With increasing longitudinal coordinate turbulization of the flow (except for the near-wall and near-axis regions) occurs, which shows up as the presence of a turbulence front and a shift of the maximum of kinetic turbulence energy from the wall into the flow (Fig. 11). Near the channel wall, a layer with vanishing small values of the kinetic turbulence energy (rejection zone) is situated. Near the permeable wall and the channel axis, the flow is practically laminar. An increase in the level of turbulent velocity pulsations is observed in the region of a strong shift at a distance from the channel wall where the liquid particles moving normally to the surface have to turn around in the narrow near-surface zone.

The level of turbulent pulsations in a permeable-wall channel is similar to the level of turbulence in a fully developed turbulent flow in the channel when the viscous and Reynolds stresses are at equilibrium with stresses caused by pressure.

The presence of a discrete component has a laminarizing effect on the flow. The kinetic turbulence energy profiles in the two-phase flow are shown in Fig. 12.

The inverse effect of impurity on the turbulence field is defined by the ratios of time micro- and macroscales of turbulence in different regions of the flow to the relaxation time of the particle. The presence of two scales in the

equations of the k–ε model of turbulence leads to a different character of the influence of the discrete component depending on the impurity inertia parameter. The turbulizing effect of small particles ($r_p \sim 1$ μm) moving practically at equilibrium with the gas is due to the decrease in the viscous dissipation. Small particles, not interacting with the energy-consuming pulsations of the gas, cause suppression of the high-frequency part of the spectrum responsible for the turbulent energy dissipation. The decrease in the kinetic turbulence energy due to the introduction of particles of diameter $r_p > 5$ μm into the flow is explained by the additional dissipation as a result of the interphase averaged and pulsation sliding.

Conclusions. Computational modeling of turbulent flows of a gas suspension in the vicinity of the critical point and in a permeable-wall channel has been performed. The results of numerical calculations permit elucidating the influence of the density and size of particles of the dispersed phase on the local (velocity and temperatures distributions and turbulence) characteristics and integral (friction and heat transfer coefficients) characteristics of the flow.

The results presented reflect the main trends and mechanisms of the processes proceeding in turbulent flows of a gas suspension and form the basis for constructing a more general model taking into account a number of additional factors and widening the range of applicability of the computational algorithm.

NOTATION

a, velocity gradient of inviscid flow, 1/sec; c, specific heat capacity, J/(kg·K); C, constant; C_f, friction coefficient; h, half-width of the channel, m; k, kinetic turbulence energy, m^2/sec^2; K, dimensionless kinetic turbulence energy; M, dimensionless parameter; Nu, Nusselt number; r, radius, m; R, characteristic size, m; Re, Reynolds number; Stk, Stokes number; x, y, coordinates; v, velocity component of viscous flow, m/sec; U, V, velocity components of inviscid flow, m/sec; α, volume concentration; ε, dissipation velocity of kinetic turbulence energy, m^2/sec^3; θ, degree of turbulence; κ, mass concentration; ν, kinematic viscosity, m^2/sec. Subscripts: g, gas; m, maximum; p, particle; w, wall; 0, pure gas.

REFERENCES

1. A. A. Shraiber, L. B. Gavin, V. A. Naumov, and V. P. Yatsenko, *Turbulent Gas Suspension Flows* [in Russian], Naukova Dumka, Kiev (1987).
2. A. Yu. Varaksin, *Turbulent Flows of a Gas with Solid Particles* [in Russian], Fizmatlit, Moscow (2003).
3. V. M. Alipchenkov and L. I. Zaichik, Modeling of turbulent motion of particles in a vertical channel, *Izv. Ross. Akad. Nauk*, *Mekh. Zhidk. Gaza*, No. 4, 50–65 (2006).
4. Q. Wang and K. D. Squires, Large eddy simulation of particle-laden turbulent channel flow, *Phys. Fluids*, **8**, No. 5, 1207–1223 (1996).
5. L. I. Zaichik and V. M. Alipchenkov, Kinetic equation for the probability density function and temperature of particles in an inhomogeneous turbulent flow, *Teplofiz. Vys. Temp.*, **36**, No. 4, 596–606 (1998).
6. J. O. Hinze, *Turbulence* [Russian translation], Fizmatlit, Moscow (1963).
7. K. N. Volkov and V. N. Emel'yanov, Calculation of turbulent two-phase flow in the region of impingement of a flow on a body, *Inzh.-Fiz. Zh.*, **71**, No. 4, 599–605 (1998).
8. K. N. Volkov and V. N. Emel'yanov, Approximate method for calculating turbulent two-phase flow in a channel with permeable walls, *Inzh.-Fiz. Zh.*, **72**, No. 5, 905–912 (1999).
9. R. M. Tracy and D. C. Willcox, Freestream turbulence effects on stagnation point heat transfer, *Raketn. Tekh. Kosmonavt.*, **13**, No. 7, 61–69 (1975).
10. S. S. Chentsov, Influence of turbulence on the heat transfer in the vicinity of the critical point, *Izv. Ross. Akad. Nauk*, *Mekh. Zhidk. Gaza*, No. 6, 52–59 (1983).
11. M. C. Smith and A. M. Kuethe, Effects of turbulence on laminar skin friction and heat transfer, *Phys. Fluids. Phys. Plasmas*, **9**, No. 12, 2337–2344 (1966).
12. A. S. Sukomel, F. F. Tsvetkov, and R. R. Kerimov, *Heat Transfer and Hydraulic Resistance in Motion of a Gas Suspension in Tubes* [in Russian], Énergiya, Moscow (1977).
13. B. A. Raizberg, B. T. Erokhin, and K. P. Samsonov, *Principles of the Theory of Working Processes in Solid-Propellant Rocket Systems* [in Russian], Mashinostroenie, Moscow (1972).